JTTEE5 9:68-72

Monoclinic Zirconia Distributions in Plasma-Sprayed Thermal Barrier Coatings

M.J. Lance, J.A. Haynes, M.K. Ferber, and W.R. Cannon

(Submitted 26 January 1999; in revised form 5 December 1999)

Phase composition in an air plasma-sprayed Y_2O_3-stabilized ZrO_2 (YSZ) top coating of a thermal barrier coating (TBC) system was characterized. Both the bulk phase content and localized pockets of monoclinic zirconia were measured with Raman spectroscopy. The starting powder consisted of ~15 vol.% monoclinic zirconia, which decreased to ~2 vol.% in the as-sprayed coating. Monoclinic zirconia was concentrated in porous pockets that were evenly distributed throughout the TBC. The pockets resulted from the presence of unmelted granules in the starting powder. The potential effect of the distributed monoclinic pockets on TBC performance is discussed.

Keywords Raman microscopy, TBC, HOSP, plasma spraying, zirconia

1. Introduction

Stabilized zirconia has been used extensively in the gas turbine industry as a thermal barrier coating (TBC), in order to protect hot-section metallic components from high temperatures. Stecura empirically determined that 6 to 8 wt.% yttria-stabilized zirconia (YSZ) results in a TBC system with the longest life.[1] This level of yttria produced deposits composed mostly of tetragonal zirconia with small percentages of monoclinic and cubic zirconia present.

Previous researchers have measured phase changes in zirconia TBCs as a function of temperature and various processing parameters. Most of these studies used x-ray diffraction to determine the phase content,[2–5] although Raman spectroscopy has also been used. Benner and Nagelberg used Raman spectroscopy to measure phase changes in electron beam-physical vapor deposition (EB-PVD) YSZ as a function of temperature.[6] Iwamoto *et al.* characterized phase transformations in plasma-sprayed YSZ TBCs after indentation using Raman spectroscopy.[2] However, none of these studies have taken advantage of the high spatial resolution of Raman microscopy to measure localized phase distributions in plasma-sprayed zirconia, as has been done on transformation-toughened zirconia around cracks.[7,8,9] In this work, we relate the bulk measurements of phase content to localized distributions of monoclinic pockets in a plasma-sprayed YSZ coating. We show that the monoclinic phase is concentrated in pockets that are evenly distributed throughout the zirconia TBC. These pockets result from the partially melted granules in the YSZ starting powder and may affect the thermomechanical stability of plasma-sprayed TBC systems.

M.J. Lance, J.A. Haynes, and **M.K. Ferber,** Oak Ridge National Laboratory, Oak Ridge, TN 37831-6068; and **W.R. Cannon,** Department of Ceramic and Materials Engineering, Rutgers University, The State University of New Jersey, Piscataway, NJ 08854-8065.

2. Experimental Procedure

2.1 Plasma-Sprayed TBCs

A nickel-based superalloy René (GEAE, Evendale, OH) N5 single crystal was machined to 2.2 cm diameter by 0.3175 cm thick disks. The substrate surfaces were grit blasted, cleaned, and vacuum plasma sprayed with Ni-22Cr-10Al-1Y (wt.%) superalloy bond coatings to a nominal thickness of 150 μm. The first 100 μm of the bond coat was deposited using atomized spherical powders with a size of 45 ± 10 μm (Praxiar NI-343), and powders of 106 ± 53 μm (Praxiar NI-211, Praxiar Thermal Spray Products, Appleton, WI) were used for the top 50 μm. The top coatings were applied by air plasma spraying (APS) 7.5 wt.% YSZ (with 1.5 wt.% Hf) to a thickness of 250 μm. The granules in the starting powder ranged in size from 11 to 106 μm (Metco 204NS, Sulzer Metco, Inc., Westbury, NY) and were formed by the proprietary hallow oven spherical particle (HOSP) process. Table 1 lists the deposition parameters for the APS top coating.[10] Both the starting powder and the coating were analyzed using scanning electron microscopy and energy dispersive spectroscopy (EDS). Prior to analyzing with Raman microscopy, the TBC buttons were vacuum infiltrated with epoxy, cut with a diamond saw, and polished to a 0.05 μm finish with colloidal silica.

2.2 Raman Microscopy

The Raman microprobe consisted of an argon-ion laser (Spectra Physics Inc., Mountain View, CA) operating at 514.5 nm, an optical microscope, a U1000 double monochromator (Instruments S.A., Edison, NJ), and a charge-coupled device (CCD) detector (EG&G, Inc., Wellesley, MA). The incident laser light is directed into the microscope, where it is then focused onto the sample. The scattered light from the sample is then collected at 180° back into the objective and directed into the monochromator, where it is dispersed and detected with the CCD camera. The laser power at the focal plane (sample surface) was 10 mW. Distributions of monoclinic content across metallographic TBC cross sections were collected with a spot size of ~3 μm. Bulk phase content was measured by defocusing the laser beam and averaging an area with a radius equal to the thickness of the zirconia top coat (200 to 250 μm). The

Table 1 Plasma spraying parameters(a)

Powder	Process	Amps	Voltage (V)	Ar flow (SLM)	H_2 flow	Distance (cm)	Flow(b) (g/min)	Traverse (cm/s)
204NS	APS	500	71	35	10	12	31	3

SLM = standard liters per minute; chamber pressure 30 mbar. Specimens were air cooled during APS with substrate temperatures not exceeding 250°C.
(a) Using Sulzer F4MB spray system. (b) Powder flow rate

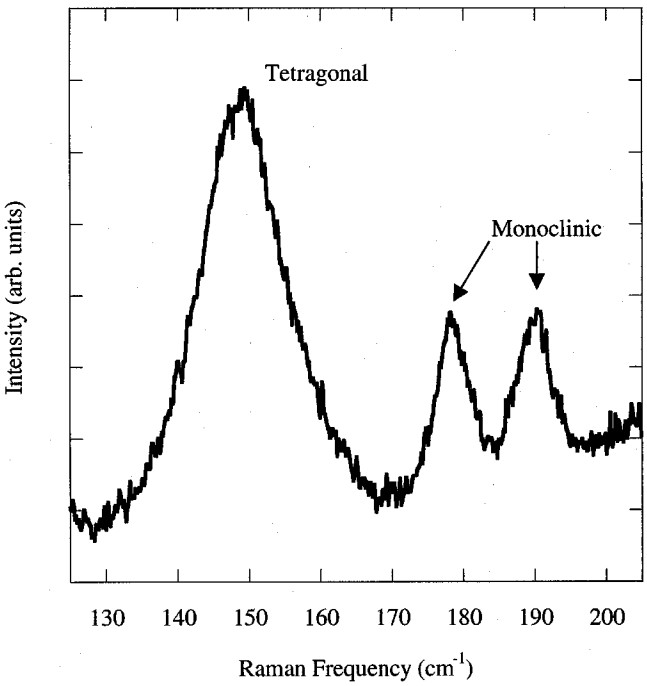

Fig. 1 Raman spectrum from a region in an APS YSZ coating with ~14 vol.% monoclinic phase. By relating the intensities of the two monoclinic peaks to the tetragonal peak, a measurement of the monoclinic content in the probed volume is obtained.

peak intensities were determined using a pseudo-Voigtian curvefit (LabCalc, Galactic Industries Corp., Salem, NH).

The intensities of the Raman peaks of a material are directly proportional to the material concentration in the probed volume.[7] This allows for the measurement of phase content in zirconia by relating the monoclinic and tetragonal peak heights through a constant that accounts for the difference in the scattering efficiency of the two phases. This constant can be obtained by measuring the intensities of the selected tetragonal and monoclinic peaks (Fig. 1) at different phase contents and plotting these intensities against one another.[9,11] The slope of this line gives the constant C in the equation

$$f_m = \frac{I_m^{180} + I_m^{190}}{C \times I_t^{147} + I_m^{180} + I_m^{190}} \quad \text{(Eq 1)}$$

where f_m is the monoclinic volume fraction and the I's are the intensities of the Raman peaks, with the subscripts and superscripts denoting the phases and peak positions, respectively. The calibration constant C in Eq 1 was measured to be 4.08, which compares well to values in the literature.[11,12] The technique is accurate to ±0.5 vol.% monoclinic zirconia.

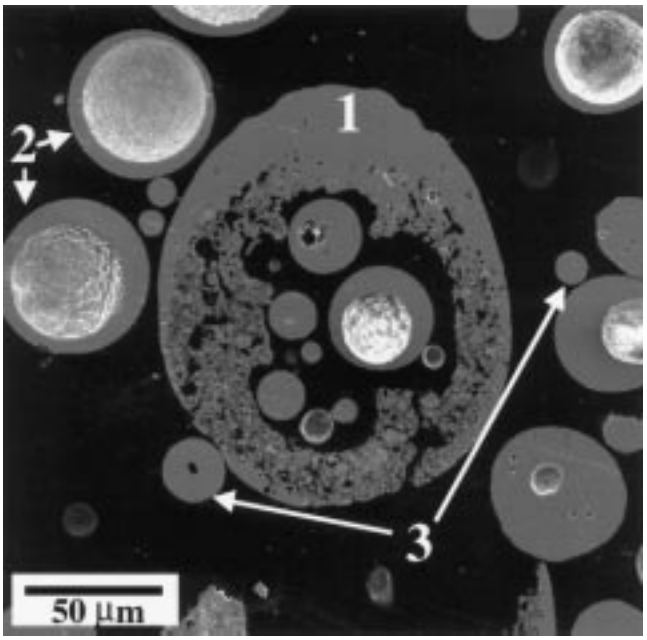

Fig. 2 The starting HOSP powder showing different types of granules.

3. Results and Discussion

The monoclinic content in the starting powder was ~15 vol.%. After plasma spraying the coating, the monoclinic content reduced to ~2 vol.%. Subsequent heating at 1150 °C for up to 200 h under both isothermal and cyclic conditions did not change the bulk phase content of the coating. A spalled zirconia flake was crushed and the percent monoclinic remained unchanged, which suggests that the APS YSZ coating does not exhibit transformation toughening during crack growth.[3,13]

The starting powder was fabricated using the HOSP process, which melts individual spray-dried agglomerates of yttria and unstabilized monoclinic zirconia using a plasma torch. One effect of the HOSP process is the formation of a solid solution of zirconia and yttria in some of the granules. Thus, the starting spray-dried powder is plasma sprayed twice to produce the final coating: first during the HOSP process, which partially stabilizes the zirconia, and again when the coating is deposited during plasma spraying. Fig. 2 shows three common types of granules found in the HOSP powder. Type 1 is a partially melted granule that consists of a porous outer shell with smaller melted particles within. These "nestlike" granules were typically larger than the other two types of granules shown in Fig. 2, averaging 82 ± 12 μm in diameter. Raman microscopy identified the porous regions to be largely monoclinic zirconia. The second type of granule is spherical and hollow, a structure that results from the expansion

of gas in the spray-dried agglomerate during the initial HOSP spraying.[14] These particles appeared to be entirely tetragonal zirconia and were of intermediate size (diameter = 70 ± 13 μm). The third type was fully solid tetragonal zirconia spheres, which were much smaller than the first two types (diameter = 29 ± 12 μm).

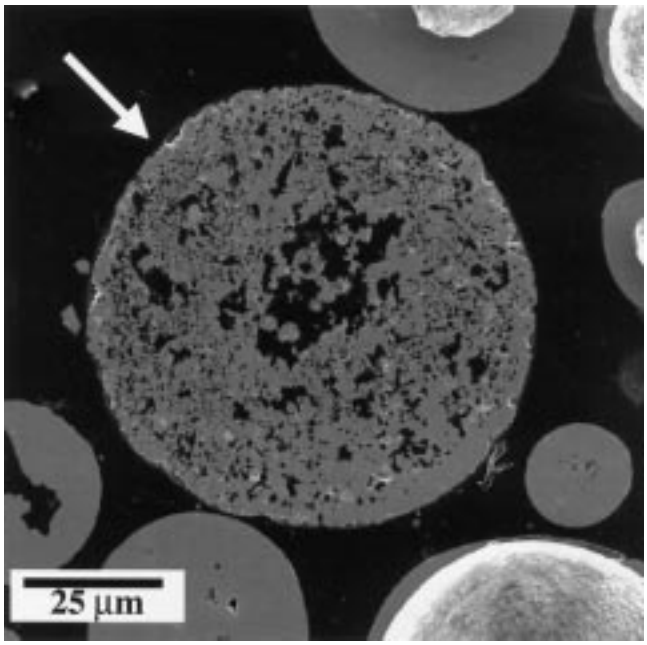

Fig. 3 A granule that was almost entirely comprised of monoclinic zirconia resulting from insufficient melting during the HOSP plasma spraying.

These granules may have melted and formed a hollow sphere at first but later collapsed due to insufficient material to form a stable shell wall.[14]

Fig. 3 shows a type 1, unmelted, monoclinic granule. Local changes in density in this granule precluded quantitative EDS to measure the elemental variations. Nevertheless, there was a larger variation in the point-to-point yttrium/zirconium concentration compared to the fully dense, melted granules. This suggests that the yttria and zirconia particles in the initial spray-dried powder had not formed a solid solution during the HOSP process. This also explains the high monoclinic content measured in these porous granules, which would result from the zirconia being unstabilized.

Monoclinic distributions were measured in the YSZ coating by focusing the laser to a ~3 μm spot size and measuring phase change along a line. One such distribution and the region it was measured along are shown in Fig. 4(a) and (b), respectively. The monoclinic content starts at ~2% near the interface but increases to ~35% about 30 μm above the interface. This spike in the percent monoclinic corresponded to a porous region in the zirconia. The change in surface roughness and density in the porous region will not affect the phase content measurement since it is only dependent upon the relative scattering efficiencies of tetragonal and monoclinic zirconia. However, the porous regions may be preferentially affected by pullout during polishing, which would reduce the amount of monoclinic content measured in these regions. Nevertheless, the monoclinic content measured in porous regions was significantly higher than that in dense regions of the coating. These porous regions were observed throughout the zirconia and were evenly distributed. They ranged in size from 10 to 30 μm and made up approximately 2% of the zirconia coating, which matches the measured bulk monoclinic content.

The monoclinic pocket from Fig. 4(b) has a microstructure similar to the type 1 granules shown in Fig. 2 and 3. The reduction

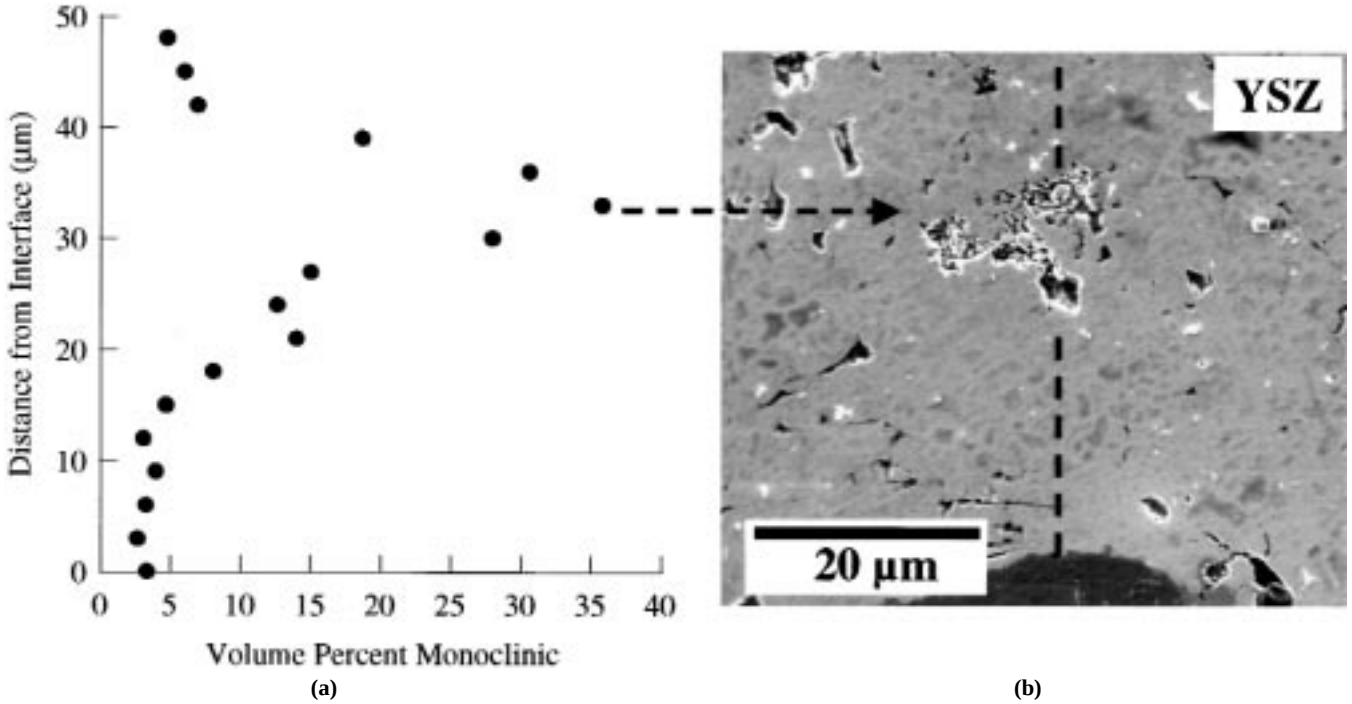

Fig. 4 The monoclinic distribution in the plasma-sprayed YSZ was measured moving away from the interface along the dashed line in (b)**.** (a) A localized high concentration of monoclinic was detected.

in the bulk monoclinic content in the powder to that in the sprayed coating results from complete melting of most of the type 1 granules, which become tetragonal zirconia splats in the coating. However, some of the monoclinic granules remain partially unmelted and result in the porous regions seen in Fig. 4(b). The amount of reduction in the monoclinic content should be determined by the plasma spraying conditions and on the dwell time of the unmelted monoclinic granules in the plasma.

Since the monoclinic pockets are very porous, they will reduce the effective stiffness of the zirconia coating, making it more strain tolerant, which will help in prolonging the life of the coating. However, if a monoclinic pocket is near the interface, it will provide no resistance to a delamination crack and in this sense may facilitate spallation. One example of this was measured on the TBC of Fig. 5(a). The monoclinic content measured along the dashed line in Fig. 5(a) is shown in Fig. 5(b). The monoclinic content increases to ~11% at the crack. The monoclinic region around this crack is not associated with a stress-induced transformation zone since no other cracks had monoclinic around them and it was shown that crushing the zirconia did not cause a phase change. Rather, the crack propagates across a monoclinic pocket that was in the zone where cracks typically propagate during TBC degradation during thermal cycling. The porous monoclinic regions would offer little resistance to crack growth.

Similar to materials toughened by microcracking, there is probably some optimum level of monoclinic pockets that will provide strain tolerance to the coating without degrading the coating by acting as stress concentrators. It would be possible to seed the starting powder with monoclinic agglomerates that would not melt during deposition. This could provide an effective and simple way to alter the elastic properties of the zirconia so as to maximize coating life.

4. Conclusions

The source of monoclinic zirconia content in a commercially available HOSP YSZ powder was determined to originate from large porous granules. These granules were only partially melted during powder fabrication and had not formed a solid solution of yttria and zirconia required to stabilize zirconia in the tetragonal phase. After plasma spraying to form a thermal barrier coating, the number of monoclinic granules decreased due to more complete melting, but those that remained resulted in ~2 vol.% porous monoclinic pockets in the YSZ coating. It was surmised that these monoclinic pockets will improve the strain tolerance of the coating but will not prevent crack growth during thermal cycling. Future work will focus on determining an optimal amount of monoclinic particles to prolong TBC life.

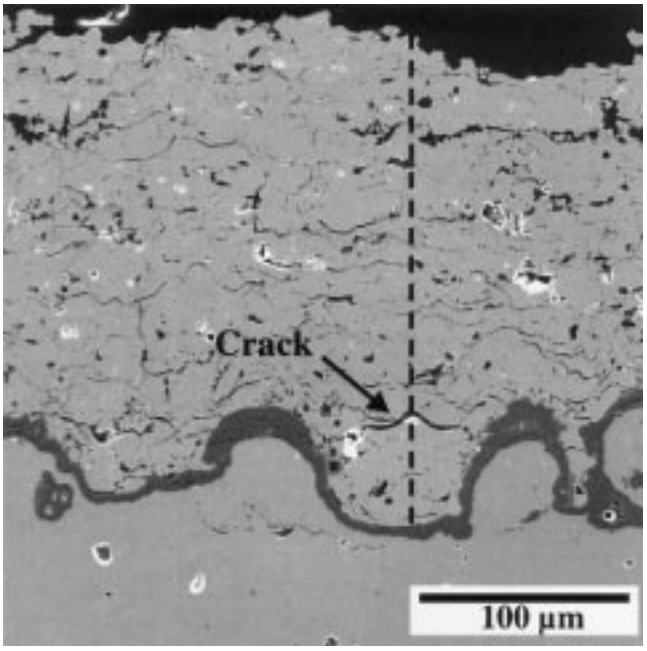

(a)

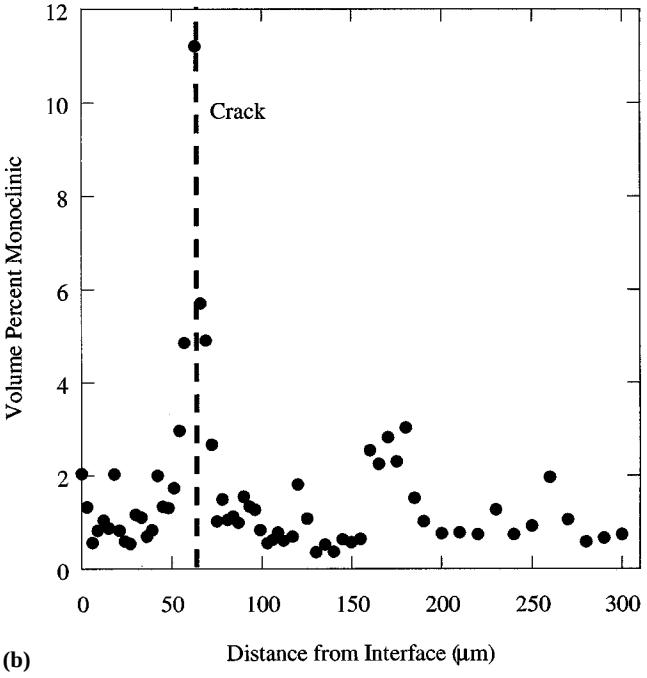

(b)

Fig. 5 (a) An APS-TBC after thermal cycling at 1150 °C and (b) the monoclinic content along the dashed line in (a). A crack has grown through a monoclinic pocket.

Acknowledgments

The authors would like to thank G. Bancke and Professor C.C. Berndt for spraying the coatings. Research was funded by the Assistant Secretary for Energy Efficiency and Renewable Energy, Office of Transportation Technologies, as part of the High Temperature Materials Laboratory Fellowship Program, and the Office of Industrial Technologies, Advanced Turbine Systems Materials Program, Oak Ridge National Laboratory, managed by Lockheed Martin Energy Research Corp. for the U.S. Department of Energy under Contract No. DE-AC05-96OR22464. M.J. Lance was funded in part by the Eugene P. Wigner Fellowship Program at Oak Ridge National Laboratory.

References

1. S. Stecura: *Adv. Ceram. Mater.*, 1986, vol. 1 (1), pp. 68-76.
2. N. Iwamoto, N. Umesaki, and S. Endo: *Thin Solid Films*, 1985, vol. 127, pp. 129-37.

3. H. Ibegazene, S. Alperine, and C. Diot: *J. Mater. Sci.*, 1995, vol. 30 (4), pp. 938-51.
4. P. Scardi, L. Lutterotti, and E. Galvanetto; *Surf. Coating Technol.*, 1993, vol. 61 (1-3), pp. 52-59.
5. N.R. Shankar, H. Herman, S.P. Singhal, and C.C. Berndt: *Thin Solid Films*, 1984, vol. 119, pp. 159-71.
6. R.E. Benner and A.S. Nagelberg: *Thin Solid Films*, 1981, vol. 84, pp. 89-94.
7. D.R. Clarke and F. Adar: *J. Am. Ceram. Soc.*, 1982, vol. 65 (6), pp. 284-88.
8. J.D. Belnap, J.F. Tsai, and D.K. Shetty: *J. Mater. Res.*, 1994, vol. 9 (12), pp. 3183-93.
9. R.H. Dauskardt, D.K. Veirs, and R.O. Ritchie: *J. Am. Ceram. Soc.*, 1989, vol. 72 (7), pp. 1124-30.
10. J.A. Haynes, M.K. Ferber, E.D. Rigney, and W.D. Porter: *Surf. Coat. Technol.* 1996, vol. 86–87, pp. 102-08.
11. G. Katagiri, H. Ishida, A. Ishitani, and T. Masaki: *Adv. Ceram.*, 1988, vol. 24, pp. 537-45.
12. M. Bowden, G.D. Dickson, D.J. Gardiner, and D.J. Wood: *J. Mater. Sci.*, 1993, vol. 28 (4), pp. 1031-36.
13. R.A. Miller, R.G. Garlick, and J.L. Smialek: *Ceram. Bull.*, 1983, vol. 62 (12), pp. 1355-58.
14. G. Pravdic and M.S.J. Gani: *J. Mater. Sci.*, 1996, vol. 31 (13), pp. 3487-95.